Chemical Physics Letters xxx (2010) xxx–xxx

Contents lists available at ScienceDirect

Chemical Physics Letters

journal homepage: www.elsevier.com/locate/cplett

OH initiated oxidation of 1,3-butadiene in the presence of O_2 and NO

Buddhadeb Ghosh, Jiho Park [1], Katie C. Anderson, Simon W. North *

Department of Chemistry, Texas A&M University, P.O. Box 30012, College Station, TX 77842, United States

ARTICLE INFO

Article history:
Received 6 April 2010
In final form 18 May 2010
Available online xxxx

ABSTRACT

The OH radical initiated oxidation of 1,3-butadiene was studied under high NOx conditions by the LP-LIF method. We report a rate constant of $(7.0 \pm 0.3) \times 10^{-11}$ s^{-1} $molecule^{-1}$ cm^3 for OH addition to 1,3-butadiene which agrees well with values reported previously. Based on the analysis of OH cycling data combined with results of earlier isomeric selective studies, we have determined a branching ratio for the major hydroxy alkyl channel to be 0.87 ± 0.08. Using this branching ratio, we have predicted the end product distribution for OH radical initiated oxidation of 1,3-butadiene and provide a condensed chemical mechanism. This study synthesizes previous work on OH initiated1,3-butadiene oxidation under high NOx conditions.

1. Introduction

1,3-Butadiene is one of the largest produced bulk chemicals [1] and is a significant atmospheric pollutant [2], carcinogen [3,4] and mutagen [5]. It is primarily an anthropogenic hydrocarbon, emitted predominantly from automobile exhaust, open burning and direct industrial emission [2]. In the atmosphere, 1,3-butadiene reacts with radical species like OH, Cl, NO_3, as well as ozone, although its atmospheric decay is dominated by reaction with OH radical [6–10]. Its atmospheric oxidation leads to the formation of ground level ozone, photochemical smog, and secondary organic aerosols [6]. 1,3-Butadiene oxidation plays an important role in determining air quality, particularly in urban areas characterized by elevated anthropogenic emissions. Developing a detailed atmospheric oxidation mechanism for 1,3-butadiene is thus critical in improving regional air quality models which serve to guides regulatory policies.

In the initial step of oxidation, the OH radical adds to 1,3-butadiene giving rise to two different hydroxy alkyl radicals (Fig. 1). This process has been studied previously and an overall rate constant of $(6.98 \pm 0.28) \times 10^{-11}$ s^{-1} $molecule^{-1}$ cm^3 has been reported [11]. The oxidative chemistry of the hydroxy alkyl radical obtained by OH addition to the outer carbon of 1,3-butadiene is distinct from the inner addition [12,13]. The outer hydroxy alkyl radical reacts with molecular oxygen by addition reaction to form a peroxy radical [13] whereas the inner hydroxy alkyl radical reacts with molecular oxygen by hydrogen abstraction mechanism to produce a C4 carbonyl compound [12]. Both reaction pathways regenerate OH radical (Fig. 2) whose concentration can be monitored using Laser Induced Fluorescence (LIF). The time dependent OH radical concentration is sensitive to the oxidation mechanism and a judicious choice of reactant concentrations, together with careful modeling, can provide quantitative insight into branching ratios. The two reaction pathways have recently been studied individually using photolytic precursors to generate the specific OH-adduct isomers [12,13]. There have also been end product studies using FTIR and mass spectrometric techniques which find acrolein, HCHO and 4-hydroxy-2-butenal as the major products [1]. However, there has been no study focused on assessment of the branching ratio between the outer and the inner hydroxy alkyl radicals. Since the two radicals have very different chemistry and lead to different final products, the initial branching is an important factor in controlling the end product distribution, and hence ozone production and the formaldehyde yield. 1,3-Butadiene has similar, yet simpler, structure and reactivity to isoprene and an understanding of the initial branching in OH-1,3-butadiene oxidation provides insight into branching in OH-isoprene oxidation which is yet to be experimentally established. We report the first OH cycling experiments performed on 1,3-butadiene and the analysis of the data, given the insight from previous isomeric selective studies, allows an estimation of the initial branching. Based on the reported branching, we predict end product yields and provide a condensed chemical mechanism for the OH-1,3-butadiene oxidation under high NOx conditions.

2. Experimental technique

The LP-LIF experiment has been explained in detail elsewhere [14,15] and only the salient features are described here. A 248 nm photolysis beam (3 mJ/cm^2) from an excimer laser (GAM laser, EX10 excimer) was used to photolyze H_2O_2 to produce OH radical. The concentration of the OH radical was monitored by

* Corresponding author.
E-mail address: swnorth@tamu.edu (S.W. North).
[1] Present Address: Department of Environmental Health, Korea National Open University, Seoul 110-791, Republic of Korea.

0009-2614/$ - see front matter © 2010 Elsevier B.V. All rights reserved.
doi:10.1016/j.cplett.2010.05.056

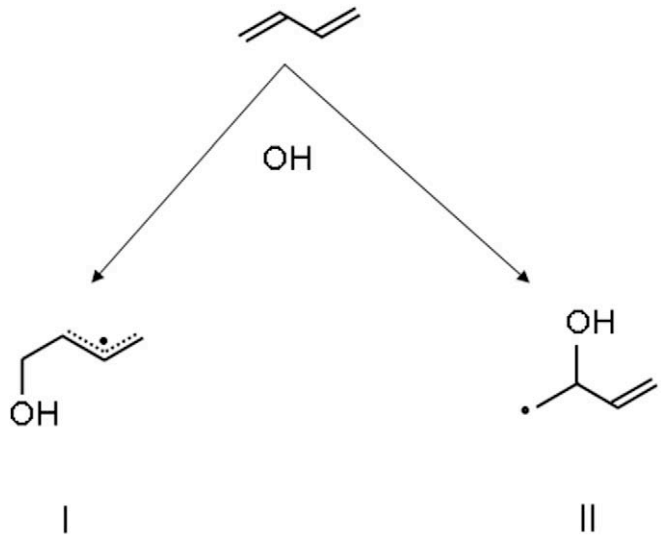

Fig. 1. Initial branching of hydroxyalkyl radicals followed by the reaction of OH radical with 1,3-butadiene.

measuring the OH fluorescence by exciting at the Q_1 (1) transition of the $A \leftarrow X$ (1, 0) band at 282 nm. The probe beam was generated by doubling the output from a dye laser (Quantel TDL-51) running Rhodamine 590 dye pumped by a 532 nm beam from an Nd YAG laser (Spectra Physics INDI). The photolysis beam and the probe beam were collinearly aligned through the LIF experiment cell. A set of lenses were used to collect the fluorescence which was detected by a photomultiplier tube (PMT) and integrated using a digital oscilloscope (Lecroy 9310A). The delay between the pump and probe lasers was controlled by a digital delay generator (SRS, DG-535). The lasers were operated at 10 Hz and each fluorescence decay was averaged over 100 laser shots. Signals were generally followed over two orders of magnitude of decay.

The reactant gases were introduced into the LIF cell through MKS flow meters and the cell was pumped down by using a mechanical pump to maintain a slow flow system where the reactant gas molecules were replenished in between every laser shot. 30% H_2O_2 (Merck) was concentrated to 90–95% by vacuum distillation and was introduced into the cell by flowing Argon through a bubbler containing the concentrated H_2O_2 at room temperature. 1,3-Butadiene (Aldrich, 99%) was purified by the freeze pump thaw technique and buffered with Ar in a 5 L bulb prior to introducing to the reaction cell to provide a typical concentration of 2×10^{14} cm^{-3}. NO (Aldrich, 98.5%) purified by passing it through ascarite to remove NO_2 and HONO and was buffered with Ar in a 5 L bulb. Typical NO concentrations were varied from 2×10^{14} cm^{-3} to 2×10^{15} cm^{-3}. Oxygen (UHP) was introduced into the reaction cell to yield concentrations in the range of 3×10^{16} cm^{-3}. The temperature of the reaction cell was maintained at room temperature (298 ± 3 K) and an MKS baratron was used to monitor the total pressure inside the cell which was buffered to 50 ± 1 torr with argon.

Table 1
A summary of the experimental conditions applied in this study.

[1,3-butadiene] 10^{14} molecules/cm^3	[NO] 10^{14} molecules/cm^3	[O_2] 10^{16} molecules/cm^3
OH + 1,3-butadiene		
1.2	0	0
2.4	0	0
3.6	0	0
4.9	0	0
7.3	0	0
OH + 1,3-butadiene + NO + O_2		
2.1	3.1	3.3
2.1	6.2	3.3
2.1	9.3	3.3
2.1	13	3.3

3. Results and discussion

In the first section, we describe the results obtained from the study of the initial reaction of OH radical with 1,3-butadiene and the determination of the rate constant. In the next section, we discuss the results of OH cycling experiments on 1,3-butadiene, and address the relative branching in between the minor and the major addition channels (Fig. 1).

3.1. OH + 1,3-butadiene reaction

The rate constant for the OH addition reaction to 1,3-butadiene was measured using LP-LIF technique. Laser photolysis of H_2O_2 at

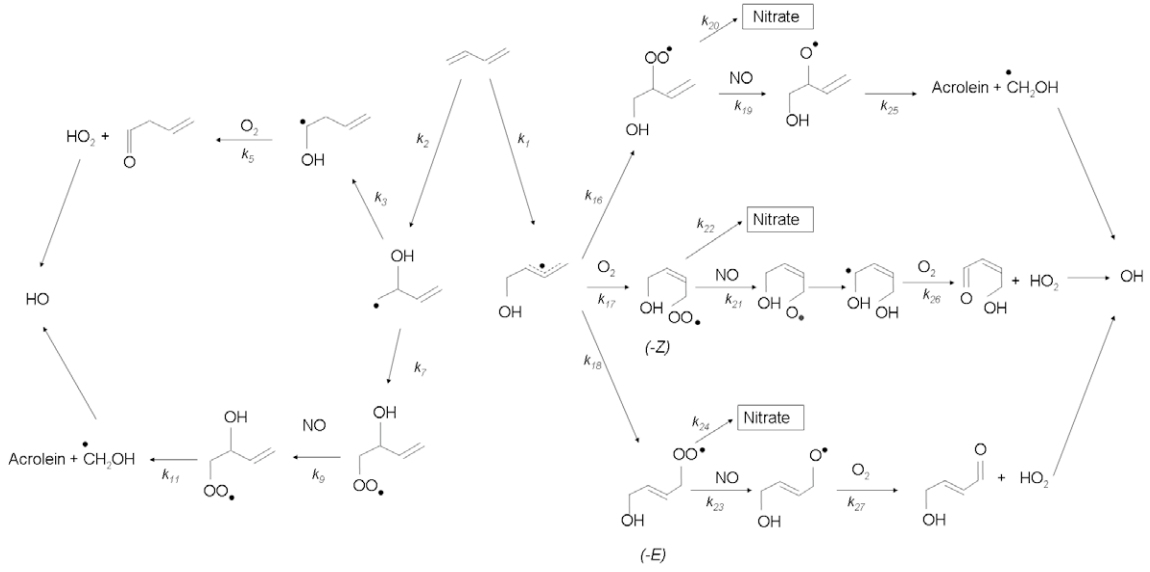

Fig. 2. Schematic diagram of OH cycling in 1,3-butadiene oxidation, for both hydroxyalkyl isomers.

248 nm results in the formation of OH and the decay of OH in the presence of 1,3-butadiene was monitored by monitoring the decay in the integrated OH fluorescence intensity using LIF technique. The concentration of H_2O_2 was typically maintained around 4×10^{13} cm^{-3} and the estimated OH concentration was typically 9×10^{10} cm^{-3} based on reported H_2O_2 absorption cross-section [16] and photolysis laser power at 248 nm. Table 1 summarizes the experimental conditions employed in this study. Fig. 3 shows OH decay curves for different concentrations of 1,3-butadiene. Pseudo first order rate constants (k^I) were obtained from the slope of the logarithmic plots. A linear least square fit of the pseudo first order rate constants versus 1,3-butadiene concentrations yields a value of $(7.0 \pm 0.3) \times 10^{-11}$ molecule^{-1} cm^3 s^{-1} for the bimolecular rate constant k^{II} (Fig. 4). The error bars correspond to 1 standard deviation from the least square regression.

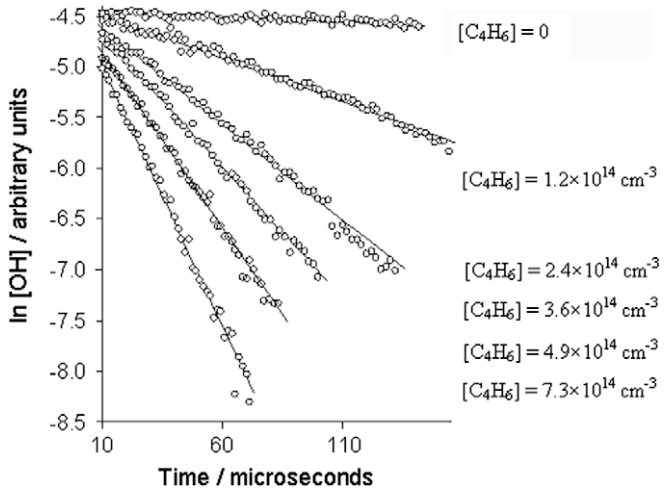

Fig. 3. Pseudo first order decays of measured OH signal for several 1,3-butadiene concentrations.

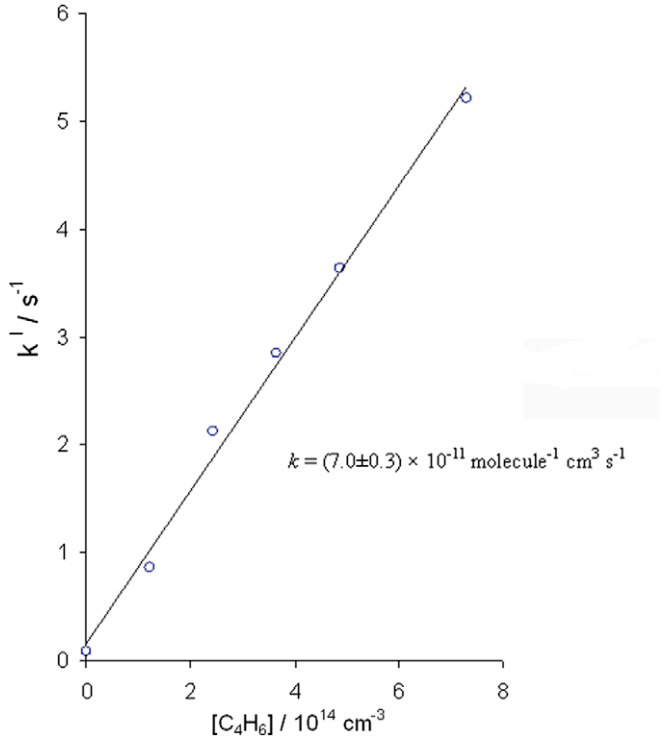

Fig. 4. Bimolecular rate constant for OH + 1,3-butadiene reaction at 50 torr, and 298 K.

This value for the rate constant is in excellent agreement with previous studies in the high pressure limit and matches a previous report of Vimal et al. [11] who used discharge flow system coupled with resonance fluorescence/laser-induced fluorescence detection of OH to obtain a value of $(6.98 \pm 0.28) \times 10^{-11}$ molecule^{-1} cm^3 s^{-1} at 300 K and 5 torr pressure. Our value is also in good agreement with values of $(6.83 \pm 0.24) \times 10^{-11}$ molecule^{-1} cm^3 s^{-1} reported at 298 K and 1 torr pressure using a relative rate discharge flow technique [7] and $(6.85 \pm 0.69) \times 10^{-11}$ molecule^{-1} cm^3 s^{-1} measured by Atkinson et al. in 50 torr of argon using the flash photolysis-resonance fluorescence technique [17]. The OH-1,3-butadiene reaction has a small negative activation energy (approximately −1 kcal/mole) and, therefore does not exhibit significant temperature dependence [7,11,17].

3.2. OH cycling from 1,3-butadiene in the presence of NO and O_2

The hydroxy alkyl radical produced by OH addition to 1,3-butadiene reacts with O_2 either by hydrogen abstraction to form a C4 carbonyl compound and HO_2 (isomer II) or by addition reaction to form a peroxy radical (isomer I) (Fig. 2). In the polluted atmosphere with high NO concentration, the peroxy radical reacts with NO to form alkoxy radical, which then either dissociate or reacts with oxygen to form different end products and HO_2. The reaction of HO_2 with NO regenerates OH radical (Fig. 2). Fig. 5 shows a representative data set obtained from OH cycling experiments at a 1,3-butadiene concentration of 2.11×10^{14} molecules cm^{-3}, $[O_2] = 3.3 \times 10^{16}$ molecules cm^{-3}, and [NO] varied from 3.1×10^{14} molecules cm^{-3} to 1.3×10^{15} molecules cm^{-3}. The circles represent the data points and the solid lines represent the best fit simulation to the data. In the absence of NO, the OH signal exhibits a pseudo first order decay with a bimolecular rate constant of $(7.0 \pm 0.3) \times 10^{-11}$ molecule^{-1} cm^3 s^{-1} due to the reaction with1,3-butadiene. In the presence of NO, the early time OH signal exhibits an exponential decay until the onset of cycling (~100 μs). At this time, the decay rate decreases due to the regeneration of OH, finally reaching steady state at long times. At higher NO concentration, OH cycling is established at earlier times and there is a long time decay due to NO termination reactions.

A numerical program Kintecus [19] was used to simulate the data using the model comprised of 33 reactions, as described in Table 2, as well as to perform sensitivity analysis. The model describes the detailed oxidative chemistry of the two hydroxy alkyl radical isomers (I and II in Fig. 1) under high NOx conditions. The distinct chemistry of these isomers has been studied previously by Greenwald et al. [12] and Ghosh et al. [13] using photolytic precursors that afford isolation of individual isomeric pathways. Both the hydroxyalkyl isomers I and II undergo a series of reactions to regenerate OH radicals, however the rate of OH cycling from isomer II is considerably faster than from isomer I. This is a result of the experimental conditions employed which ensures that the rate determining step for OH regeneration from isomer II (k_5 [O_2]) is faster than that from isomer I (k_{19} [NO]). A higher branching ratio for isomer II will thus result in greater OH cycling, affecting the shape of the OH concentration time profile. The main focus of current study was to determine the relative contribution of these two isomeric pathways, i.e. the relative branching ratios of the rate constants k_1 and k_2. We find that small changes in the branching ratio between these two rate constants have a profound effect on the simulations. The other rate constants have been fixed to values reported previously by Ghosh et al. [13] and Greenwald et al. [12] Thus we employed only a single parameter in the simulation, the relative branching between k_1 and k_2. The most satisfactory fit to the experimental data was obtained for a branching ratio of 0.87

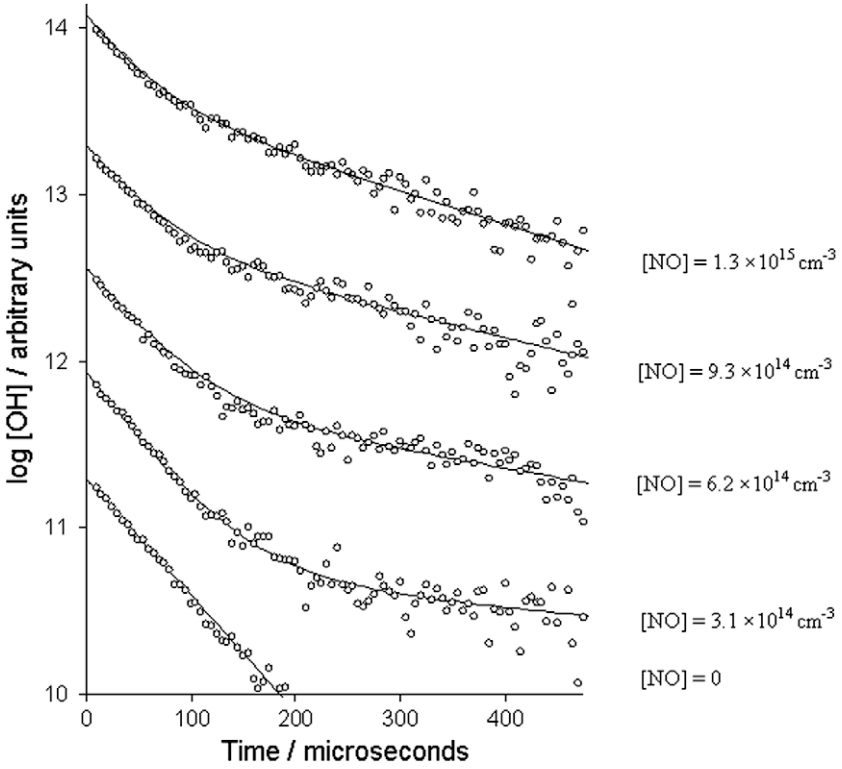

Fig. 5. OH decays at different NO concentrations. Circles represent experimental data, and lines represent the fits using the reaction mechanism and rate constants in Table 2 with $[C_4H_6] = 2.11 \times 10^{14}$ cm^{-3} and $[O_2] = 3.27 \times 10^{16}$ cm^{-3}.

Table 2
Reaction Mechanism and Corresponding Rate Constants (298 K) used for simulation of the experimental data.

Reaction			Rate Constant	Ref.	Comment
k_1	$C_4H_6 + HO \rightarrow$	1-HOC_4H_6	6.1×10^{-11}	[a]	Radicals I and II branching(Fig. 1)
k_2	$C_4H_6 + HO \rightarrow$	2-HOC_4H_6	0.9×10^{-11}	[a]	
k_3	2-$HOC_4H_6 \rightarrow$	Alpha-HOC_4H_6	7×10^{-11}	[12]	Oxidation chemistry of hydroxy alkyl radical II (Fig. 2)
k_4	2-$HOC_4H_6 \rightarrow$	Beta-HOC_4H_6	3×10^{-11}	[12]	
k_5	Alpha-$HOC_4H_6 + O_2 \rightarrow$	Alpha-$OC_4H_6 + HO_2$	3.3×10^{-11}	[12]	
k_6	Alpha-$HOC_4H_6 + NO \rightarrow$	Alpha-HOC_4H_6NO	2.2×10^{-11}	[12]	
k_7	Beta-$HOC_4H_6 + O_2 \rightarrow$	Beta-$OHC_4H_6O_2$	2.3×10^{-12}	[12]	
k_8	Beta-$HOC_4H_6 + NO \rightarrow$	Beta-HOC_4H_6NO	2.2×10^{-11}	[12]	
k_9	Beta-$OHC_4H_6O_2 + NO \rightarrow$	Beta-$OHC_4H_6O + NO_2$	1.4×10^{-11}	[12]	
k_{10}	Beta-$OHC_4H_6O_2 + NO \rightarrow$	Beta-$OHC_4H_6ONO_2$	8.4×10^{-13}	[12]	
k_{11}	Beta-$OHC_4H_6O \rightarrow$	$HCHO + OHC_3H_4$	Prompt	[12]	
k_{12}	Beta-$OHC_4H_6O + NO \rightarrow$	Beta-OHC_4H_6ONO	3×10^{-11}	[12]	
k_{13}	$OHC_3H_4 + O_2 \rightarrow$	$OC_3H_4 + HO_2$	3×10^{-11}	[12]	
k_{14}	$OHC_3H_4 + NO \rightarrow$	OHC_3H_4NO	3×10^{-11}	[12]	
k_{15}	1-$HOC_4H_6 + NO \rightarrow$	1-HOC_4H_6NO	2.0×10^{-11}	[13]	Oxidation chemistry of hydroxy alkyl radical I (Fig. 2)
k_{16}	1-$HOC_4H_6 + O_2 \rightarrow$	β-$HOC_4H_6O_2$	5.25×10^{-13}	[13]	
k_{17}	$HOC_4H_6 + O_2 \rightarrow$	Z-$HOC_4H_6O_2$	8.75×10^{-14}	[13]	
k_{18}	$HOC_4H_6 + O_2 \rightarrow$	E-$HOC_4H_6O_2$	8.75×10^{-14}	[13]	
k_{19}	β-$HOC_4H_6O_2 + NO \rightarrow$	β-$HOC_4H_6O + NO_2$	1.4×10^{-11}	[13]	
k_{20}	β-$HOC_4H_6O_2 + NO \rightarrow$	β-$HOC_4H_6ONO_2$	8.4×10^{-13}	[13]	
k_{21}	Z-$HOC_4H_6O_2 + NO \rightarrow$	Z-$OHC_4H_5OH + NO_2$	1.4×10^{-11}	[13]	
k_{22}	Z-$HOC_4H_6O_2 + NO \rightarrow$	Z-$HOC_4H_6ONO_2$	8.4×10^{-13}	[13]	
k_{23}	E-$HOC_4H_6O_2 + NO \rightarrow$	E-$OHC_4H_6O + NO_2$	1.4×10^{-11}	[13]	
k_{24}	E-$HOC_4H_6O_2 + NO \rightarrow$	E-$HOC_4H_6ONO_2$	8.4×10^{-13}	[13]	
k_{25}	β-$HOC_4H_6O \rightarrow$	$CH_2OH + OC_3H_4$	Prompt	[13]	
k_{26}	Z-$OHC_4H_5OH + O_2 \rightarrow$	$HO_2 + OC_4H_5OH$	1.0×10^{-11}	[13]	
k_{27}	Z-$OHC_4H_5OH + NO \rightarrow$	Z-OHC_4H_5OHNO	3.0×10^{-11}	[13]	
k_{28}	E-$HOC_4H_6O + O_2 \rightarrow$	E-$OHC_4H_5O + HO_2$	1.0×10^{-11}	[13]	
k_{29}	E-$HOC_4H_6O + NO \rightarrow$	E-HOC_4H_6ONO	3.0×10^{-11}	[13]	
k_{30}	$CH_2OH + O_2 \rightarrow$	$CH_2O + HO_2$	9.8×10^{-12}	[13]	
k_{31}	$CH_2OH + NO \rightarrow$	CH_2OHNO	1.2×10^{-11}	[13]	
k_{32}	$HO_2 + NO \rightarrow$	$OH + NO_2$	1.2×10^{-11}	[18]	
k_{33}	$OH + NO \rightarrow$	HONO	9.4×10^{-13}	[16]	

Please cite this article in press as: B. Ghosh et al., Chem. Phys. Lett. (2010), doi:10.1016/j.cplett.2010.05.056

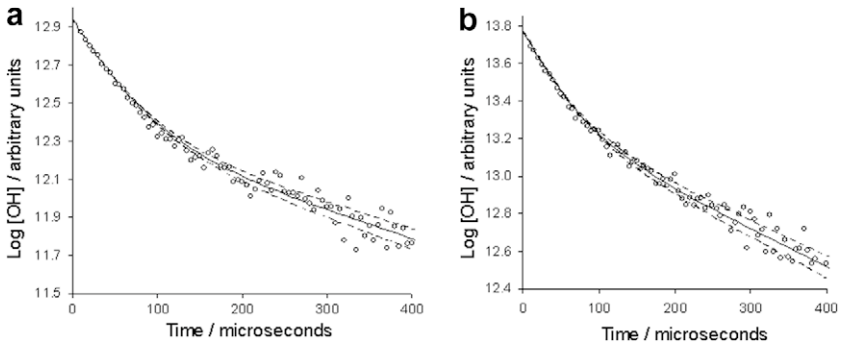

Fig. 6. OH decays at different NO concentrations. Circles represent experimental data, solid lines represent the best fits using a branching of 0.87 for the radical I. Dashed lines indicate the estimated error range for the initial branching in between the outer and inner isomers (k_1 and k_2). The outer branching is founded to be 0.87 ± 0.08 (A) $[C_4H_6] = 2.11 \times 10^{14}$ cm^{-3}, $[O_2] = 3.27 \times 10^{16}$ cm^{-3}, $[NO] = 9.3 \times 10^{14}$ cm^{-3}; (B) $[C_4H_6] = 2.11 \times 10^{14}$ cm^{-3}, $[O_2] = 3.27 \times 10^{16}$ cm^{-3}, $[NO] = 1.5 \times 10^{15}$ cm^{-3}.

for k_1. An error analysis of this simulation to data provides an estimated error range of ±0.08 for the branching of the outer channel which represents two standard deviations. The error analysis focused on the data points in the time interval 125–400 μs as the branching between the inner and the outer isomers (k_1 and k_2) has the greatest sensitivity for this interval. Fig. 6 shows the best fit obtained for the OH cycling data with a yield of 87% for isomer I and the corresponding error limit of ±8%. There has been only one other estimation of this branching, reported by Jenkin et al. [20]. Based on their study of peroxy radical kinetics using laser flash photolysis/UV absorption spectrometry, they estimated a branching of 0.87 for the radical I channel, in close agreement with our value.

4. Predicted end product distribution

Based on the branching of 0.87:0.13 for isomers I and II, we can predict end product yields given the chemistry of the individual radical pathways [12,13]. The outer and inner OH-1,3-butadiene adducts undergo different types of chemistry. A major fraction of the inner adduct undergo an isomerization to form α-hydroxyalkyl radicals (k_3), which react with O_2 via hydrogen abstraction to form the C4 carbonyl compound, while a minor fraction undergoes O_2 addition to form β-peroxy radicals (k_7), which react with NO to ultimately form acrolein and HCHO (k_{11}). The outer adduct reacts via oxygen addition to form β, Z-δ and E-δ peroxy isomers (k_{16}, k_{17}, and k_{18}), which further undergo reaction with NO to form alkoxy compounds (k_{19}, k_{21}, and k_{23}), and finally produce acrolein (k_{25}) and 4-hydroxy-2-butenal (k_{25}, k_{26}, and k_{27}) as first generation end products. The chemistry is schematically described in Fig. 2, and the end product distribution is presented in Table 3.

The estimated product yields for organic nitrate, acrolein, 4-hydroxy-2-butenal, 3-butenal (C_4 carbonyl) and HCHO are 6%, (64 ± 12)%, (21 ± 11)%, (9 ± 6)%, and (64 ± 12)%. These product yields are well within the range of the values reported in previous product studies [1,10,21,22]. Our study was insensitive to the nitrate yield and we have used value reported in the literature [1]. Our acrolein yield is within the range of (54–69)% as reported in the literature [1,10,21]. Our reported acrolein yield is slightly higher than the yields of (59 ± 6)% and (58 ± 4)%, as reported by Berndt et al. [1] and Tuazon et al. [10] respectively, is similar to their reported HCHO yields of (62 ± 5)% and (64 ± 8)%. Since HCHO and acrolein are co-product of the same reaction, they should be formed in equal yields. From their 'wall less' experiments, Sprengnether and co-workers reported equal yield for acrolein and HCHO at lower pressure (445 torr), and slightly higher HCHO yields at higher pressure (750 torr) [21]. Our reported yield of (21 ± 11)% for 4-hydroxy-2-butenal matches very well with the only two others reported yields of 23.0 ± 10 and 25^{+15}_{-10} as determined by Berndt et al. [1] and Baker et al. [22], respectively. The C_4 carbonyl 3-butenal, to our knowledge, has never been reported; however its C5 analogue has been reported in case of isoprene oxidation [23]. End product analysis studies account for about 80–90% of carbon balance in the OH initiated oxidation of 1,3-butadiene [1] and we believe that the C4 carbonyl compound may account for some of the missing carbon balance. Based on our current understanding, we can build a condensed chemical mechanism for OH radical initiated oxidation of 1,3-butadiene under high NOx conditions.

$$1,3\text{-Butadiene} + OH = 0.06\ RONO_2 + 0.64\ \text{Acrolein} + 0.3\ BUPD + 0.64\ HCHO + 0.94\ HO_2 + 0.85\ NO_2$$

where, $RONO_2$ = organic nitrate (assuming 6% nitrate yield), BUPD = first generation products other than acrolein = C4 carbonyl (9%), 4-hydroxy-2-butenal (21%), NO_2 = total NO_2 formed from NO.

5. Conclusion

The OH radical initiated oxidation of 1,3-butadiene was studied in high NOx condition by using LP-LIF technique. The rate constant for the reaction of OH radical with 1,3-butadiene was measured to be $(7.0 \pm 0.3) \times 10^{-11}$ s^{-1} molecule^{-1} cm^3. Analysis of OH cycling

Table 3
Summary of end product distributions (in percentage yield) predicted by using the branching ratio of 0.87 ± 0.08:0.13 ± 0.08 for outer: inner addition channel, as determined in current study and using the previously reported chemistries of these isomeric channels (Fig. 1). Included for comparison are the end product distributions reported in other studies.

End product	Current study	Tuazon [10]	Sprengnether [21]		Berndt [1]	Baker [22]
			445 torr	750 torr		
Acrolein	64 ± 12	58 ± 4	69 ± 7	54	59 ± 6	58 ± 10
4-Hydroxy-2-butenal	21 ± 11				23 ± 10	25^{+15}_{-10}
HCHO	64 ± 12	62 ± 5	69 ± 10	58	64 ± 8	

Please cite this article in press as: B. Ghosh et al., Chem. Phys. Lett. (2010), doi:10.1016/j.cplett.2010.05.056

experiments permits the determination of the branching in between the outer and inner OH-1,3-butadiene adduct isomers. The branching of the outer isomeric channel was found to be 0.87 ± 0.08. The current study provides a comprehensive model for oxidation of 1,3-butadiene under high NOx condition, and the model was used to predict the distribution of the first generation end products.

Acknowledgment

This work was supported by the Environmental Protection Agency (EPA) and Texas Commission on Environmental Quality (TCEQ).

References

[1] T. Berndt, O. Boge, J. Phys. Chem. A 111 (2007) 12099.
[2] United States Environmental Protection Agency, Locating and Estimating Air Emissions from Sources of 1, EPA-454/R-96-008; Office of Air Quality Planning and Standards: Research Triangle Park, NC, 1996.
[3] I.L. Cote, S.P. Bayard, Environ. Health Perspect. 86 (1990) 149.
[4] United States Environmental Protection Agency, Health Assessment of 1, EPA/600/P-98/001F; Office of Research and Development: Washington, DC, 2002.
[5] A.D. Kligerman, C.L. Doerr, V.S. Milholland, A.H. Tennant, Toxicology 113 (1996) 336.
[6] G.J. Dollard, C.J. Dore, M.E. Jenkin, Ambient Concentrations of 1,3-Butadiene in the UK, Elsevier Science, Ireland Ltd., 2001, p. 177.
[7] Z.J. Li, P. Nguyen, M.F. de Leon, J.H. Wang, K.L. Han, G.Z. He, J. Phys. Chem. A 110 (2006) 2698.
[8] X.Y. Liu, H.E. Jeffries, K.G. Sexton, Atmos. Environ. 33 (1999) 3005.
[9] A. Notario, G. Le Bras, A. Mellouki, Chem. Phys. Lett. 281 (1997) 421.
[10] E.C. Tuazon, A. Alvarado, S.M. Aschmann, R. Atkinson, J. Arey, Environ. Sci. Technol. 33 (1999) 3586.
[11] D. Vimal, A.B. Pacheco, S.S. Iyengar, P.S. Stevens, J. Phys. Chem. A 112 (2008) 7227.
[12] E.E. Greenwald et al., J. Phys. Chem. A 109 (2005) 7915.
[13] B. Ghosh, A. Bugarin, B.T. Connel, S.W. North, J. Phys. Chem. A 114 (2010) 5299.
[14] W.S. McGivern, I. Suh, A.D. Clinkenbeard, R. Zhang, S.W. North, J. Phys. Chem. A 104 (2000) 6609.
[15] J.E. Reitz, W.S. McGivern, M.C. Church, M.D. Wilson, S.W. North, Int. J. Chem. Kinet. 34 (2002) 255.
[16] W.B. DeMore, S.P. Sander, D.M. Golden, R.F. Hampson, M.J. Kurylo, C.J. Howard, A.R. Ravishankara, C.E. Kolb, M.J. Molina, Chemical Kinetics and Photochemical Data for Use in Stratospheric Modeling, JPL Publication 02-25; Jet Propulsion Lab: Pasadena, CA, 2003.
[17] R. Atkinson, R.A. Perry, J.N. Pitts, J. Chem. Phys. 67 (1977) 3170.
[18] I. Glaschickschimpf, A. Leiss, P.B. Monkhouse, U. Schurath, K.H. Becker, E.H. Fink, Chem. Phys. Lett. 67 (1979) 318.
[19] J.C. Ianni, Kintecus Windows, Version 2.80, 2002.
[20] M.E. Jenkin, A.A. Boyd, R. Lesclaux, J. Atmos. Chem. 29 (1998) 267.
[21] M. Sprengnether, K.L. Demerjian, N.M. Donahue, J.G. Anderson, J. Geophys. Res. Atmos. 107 (2002) 13.
[22] J. Baker, J. Arey, R. Atkinson, Environ. Sci. Technol. 39 (2005) 4091.
[23] E.E. Greenwald et al., J. Phys. Chem. A 114 (2010) 904.